IJICTR
International Journal of Information & Communication Technology Research

Volume 14- Number 1 – 2022 (13 -24)

Spectral and Energy Efficiency Wireless-Powered Massive-MIMO Heterogeneous Network

Sepideh Haghgoy
Faculty of Engineering
SKU University
Shahrekord, Iran
haghgoy@stu.sku.ac.ir

Mohammadali Mohammadi*
Faculty of Engineering
SKU University
Shahrekord, Iran
m.a.mohammadi@sku.ac.ir

Zahra Mobini
Faculty of Engineering
SKU University
Shahrekord, Iran
z.mobini@sku.ac.ir

Received: 27 November 2021 – Revised: 24 January 2022 - Accepted: 9 February 2022

Abstract— **In this paper, we study the spectral efficiency (SE) and energy efficiency (EE) of wireless-powered full-duplex (FD) heterogeneous networks (HetNets). In particular, we consider a two-tire HetNet with half duplex (HD) massive multiple-input multiple-output (MIMO) macrocell base stations (MBSs), FD small cell base stations (SBSs) and FD user equipments (UEs). UEs rely on energy harvesting (EH) from radio frequency signals to charge their batteries for communication with serving base stations. During the energy harvesting phase, UEs are associated to MBSs/SBSs based on the mean maximum received power (MMP) scheme. In the consecutive data transmission phase, each UE downloads packets from the same MBSs/SBSs, while uploads packets to the nearest SBSs using the harvested energy. We use tools from stochastic geometry to develop an analytical framework for the average UL power transfer and the UL and DL coverage probability analysis. We further investigate the EE of the proposed DUDe scheme to demonstrate the impact of different system parameters on the EE. Finally, we validate the analytical results through simulation and discuss the significance of the proposed DUDe user association to improve the average DL and UL SE in the wireless-powered FD HetNets.**

Keywords: component; Heterogeneous networks, decoupled user association, full-duplex communications, energy harvesting, energy efficiency.

Article type: Research Article

Publisher: ICT Research Institute

I. INTRODUCTION

Improving the spectral efficiency (SE) of the wireless networks is viewed as the primary driving factor behind the growth of wireless communications, particularly when new technologies such as the Internet-of-Things (IoT), augmented reality, haptic applications, mature [1]. The IoT has been recognized as a promising technology for the fifth generation (5G) and beyond mobile communication networks [2]–[4]. IoT enables information exchange among heterogeneous applications and millions of devices.

* Corresponding Author

However, in practice, implementation of IoT imposes strict limitations on energy and cost [4]. Therefore, supplying energy to a large number of heterogeneous IoT devices is a substantial challenge. Radio frequency energy harvesting (RF-EH) which exploits the available RF to power the wireless devices has been recently emerged as a promising technology for future wireless networks, including the IoT [5]. Moreover, form the energy efficiency (EE) point of view, RF-EH has been considered as a promising solution [6]. On the other hand, deployment of low power small cells, (SCells), such as femtocell and picocell can improve the coverage and capacity of cellular networks by exploiting spatial reuse of the spectrum [3]. Therefore, heterogeneous networks (HetNets) have triggered significant interest in research and industry due to their potential to meet the ever-increasing demands of future wireless Networks. In HetNets, divers set of SCells with various applications overlaid on top of the macrocell (MCell).

Full-duplex (FD) communication, which allows simultaneous transmission and reception over the same frequency band, has been widely applied in HetNets to further improve the SE of the network [7]–[10]. FD transceivers suffer for the self-interference (SI), caused by power leakage from the transmitter to receiver [11]-[13]. Due to the simultaneous operation of uplink (UL) and downlink (DL) user equipments (UEs) in the SCell, FD communication introduces inter-node interference into the network. Therefore, new technical challenges for user association in FD-enabled HetNets emerge due to complicated interference scenarios, significant disparity in the transmit power of different BSs, and non-uniform traffic loads of different BSs in both the DL and UL transmissions. In other words, in FD HetNets, the traditional/coupled association scheme is inefficient, because it uses the same user association criterion (e.g., DL maximum received signal power) for both UL and DL transmissions. As a result, for 5G wireless communication systems, the concept of DL-UL decoupled (DUDe) user association has been proposed [14]. According to the DUDe scheme, each FD UE can receive data from one BS in DL and upload it packet to another BS in UL. Due to its promising gains over the coupled user association schemes, performance of DUDe in FD HetNets has been investigated in [15]–[20]. In two-tire cellular networks, a landmark simulation study in [16] revealed that DUDe might outperform the coupled association method. Using stochastic geometry, the authors in [16] investigated the performance of the DUDe user association in multi-tier FD networks. In [17], the work in [16] was expanded to two-tier HetNets with multi-antenna BSs. A contract theory-based distributed strategy for decoupled user association in FD cellular networks has been developed in [18]. In [19], the authors presented an optimization approach for frequency allocation and power regulation in the HetNets with DUDe to increase the quality of service per UE. In [20], a novel transmission system for a two-tier multi-cell HetNet with DUDe was presented to decrease pilot contamination and intra-cell interference. While DUDe is a widely research area in context of FD HetNets, to our best knowledge, DUDe in wireless-powered FD HetNets is still in its infancy.

In order to bridge this gap, in this paper, we focus on the DUDe user association in two-tier multi-cell HetNets, where each UE first harvests the energy from its serving BS (as a dedicated RF energy source) in the DL and utilizes the harvested energy for wireless information transfer (WIT) in the UL. In summary, the contributions of this work are as follows:

- We propose a novel DUDe user association scheme based on which UEs can associate with the serving BS in DL according to the mean maximum received power (MMP) scheme and nearest BS (NB) in UL.
- By leveraging tools from stochastic geometry, we analyze the average UL power transfer for typical UE associated with MCell base station (MBS) or SCell base station (SBS). We also derive closed-form expressions for the UL and DL coverage probabilities and area spectral efficiency (ASE) of the proposed DUDe. Furthermore, we characterize the EE for UL transmission in order to determine the effectiveness of EH by UEs. These expressions are general enough to study the impact of system parameters on performance and simple enough to evaluate with common scientific software.
- Our findings show that as the density of the SBS increases, the DL and UL coverage probability of the system increases first and then start to decreases. As a result, there is an optimum value for SBS density in the network that maximizes the probability of DL and UL coverage. This observations is in contrary to the FD HetNets without wireless power transfer (WPT) counterpart, where the DL coverage continuously increases and the UL coverage decrease.

Notation: We use $\mathrm{E}\{X\}$ to denote the expected value of the random variable (RV) X; $X \sim \exp(\mu)$ denotes RV X is exponentially distributed with mean μ; $X \sim \mathrm{Gamma}(\vartheta,\theta)$ denotes the Gamma distribution with shape ϑ and scale parameter θ, $\Gamma(a,x)$ is upper incomplete Gamma function [21, Eq. (8.350)]; ${}_2F_1(\cdot,\cdot;\cdot;\cdot)$ denotes Gauss hypergeometric function [21, Eq. (9.111)].

II. System Model

A. Network Topology

We consider two-tier FD HetNet consisting of MBSs, SBSs, and UEs, as shown in Fig. 1. The location of the MBSs, SBSs and UEs are modeled as independent homogeneous Poisson point process (HPPP), Φ_M, Φ_S and Φ_u with density λ_M, λ_S and λ_u respectively. Let $\Phi_M \sim \{X_{M,i} \in \mathbb{R}^2, i \in \mathbb{N}_+\}$, $\Phi_S \sim \{X_{S,i}$

$\in \mathbb{R}^2, i \in \mathbb{N}_+\}$ and $\Phi_u \triangleq \{X_{u_j} \in \mathbb{R}^2, i \in \mathbb{N}_+\}$ where $X_{M,i}$ and $X_{S,i}$ denote MBS and SBS i in the first and second tier and their location, respectively, and X_{u_j} denotes the location of UE j. We assume that, each MBS is equipped with a massive antenna array with N antennas, operating in HD and serves S UEs in DL. Moreover, each SBS has two antennas and operates in FD mode. The MBS and SBS transmit power are represented by P_M and P_S, respectively, where $P_M > P_S$. Furthermore, $\mathrm{E}\{P_{U_j}\}$ denotes the average transmit power of UE j. Each UE can perform either

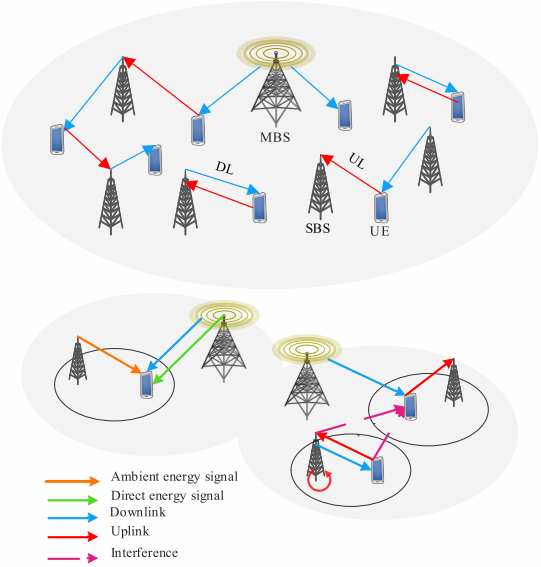

Fig. 1. System model of the two-tier HetNet.

HD or FD depending on requirement, i.e., if it wishes to exchange data with its associated BS it performs the FD mode; otherwise it operates in the HD mode.

B. User Association

We consider a frame-based transmission, where each frame is divided into two phases: DL WPT phase, and UL-DL WIT phase. During the DL WPT, each UE harvests energy from its serving BS. Accordingly, during the UL-DL WIT, UEs utilize the harvested energy for UL data transmission, while receiving information from the serving BS [22]. It should be noted that the UEs can only associate with the FD SBSs for the UL transmission due to FD capability of the SBSs. We assume that for DL data reception, each UE is associated to the same BS, as that associated with during the DL WPT phase, while in the UL it can associate to a different BS, as shown in Fig. 1.

We consider the MMP user association scheme in the DL transmission to achieve the strongest received power. In this scheme each UE is associated to a BS (MBS/SBS) that provide it with mean maximum received power. We term this user association scheme as the MMP association (MMPA) scheme [23], [24].

For the UL transmission we apply the nearest BS association (NBA) scheme to maximize the UL SINR [7], [12]. This scheme only characterizes the path loss between SBS $X_{S,i}$ and typical UE X_{u_0}. Therefore, UEs are associated with their nearest SBS.

C. Signal Transmission Model

Assume that T is the duration of one frame. During the first fraction τ, $(0<\tau<1)$ of the time frame, i.e., DL WPT phase, UEs harvest power from the received RF signals. Then during the consequent phase of duration $(1-\tau)$, UEs receive the data from MBSs/SBSs in the DL and transmit data to SBSs in UL link.

D. Energy Harvesting Phase

We assume that each UE has a large energy storage capacity, allowing for sufficient harvest energy to support a stable transmit power [25]. Furthermore, all RF signals are interpreted as energy sources, for RF-EH. Therefore, in the MCell, we adopt the simplest linear MRT beamforming to direct RF signal toward intended UEs. During τ fraction of each time slot, which is devoted to the DL WPT phase, the total harvested energy at a typical UE associated with the MBS is given by

$$E_{M,0} = \underbrace{\eta P_M \mathbf{g}_{M,0} \left\| X_{M,0} \right\|^{-\alpha_M} \tau T}_{E^1_{M,0}} + \underbrace{\eta \left(I_{M,1} + I_{S,1} \right) \tau T}_{E^2_{M,0}}, \tag{1}$$

where $E^1_{M,0}$ is the energy from the directed WPT, $E^2_{M,0}$ is the energy from the ambient RF. Here $0<\eta<1$ is the RF-to-DC conversion efficiency, $\mathbf{g}_{M,0} \sim \mathrm{Gamma}(N+S-1)$ is the small-scale fading channel power gain between MBS, $X_{M,0}$, and typical UE located at the origin, and $\|X_{M,0}\|$ denotes the distance between MBS, $X_{M,0}$, and typical UE. In addition,

$$I_{M,1} = \sum_{X_{M,i} \in \Phi_{M}/X_{M,0}} P_M \mathbf{g}_{M,i} \left\| X_{M,i} \right\|^{-\alpha_M}, \tag{2}$$

is the sum of interference from the interfering MBSs, where $\mathbf{g}_{M,i} \sim \mathrm{Gamma}(1,1)$ and $\|X_{M,i}\|$ denote, the small-scale fading interfering channel gain and the distance between a typical UE and other MBS, respectively. Furthermore,

$$I_{S,1} = \sum_{X_{S,i} \in \Phi_S} P_S g_{S,i} \left\| X_{S,i} \right\|^{-\alpha_s}, \tag{3}$$

is the sum of interference from the SBSs, where $g_{S,i} \sim \exp(1)$ and $\|X_{S,i}\|$ are, respectively, the small-scale fading interfering channel power gain and the distance between a typical UE and SBS.

Moreover, the harvested energy at a typical UE associated with the SBS can be written as

$$E_{S,0} = \underbrace{\eta P_S g_{S,0} \left\| X_{S,0} \right\|^{-\alpha_s} \tau T}_{E^1_{S,0}} + \underbrace{\eta \left(I_{M,2} + I_{S,2} \right) \tau T}_{E^2_{S,0}}, \tag{4}$$

where $E^1_{S,0}$ is the energy from the directed WPT, $E^2_{S,0}$ is the energy from the ambient RF, $g_{S,0} \sim \exp(1)$ and $\|X_{S,0}\|$ are the small-scale fading channel power gain and the distance between a typical UE and its associated

SBS, respectively. Moreover, similar to (1), the interference terms in (4) can be expressed as

$$I_{M,2} = \sum_{X_{M,i} \in \Phi_M} P_M \mathbf{g}_{M,i} \left\| X_{M,i} \right\|^{-\alpha_M}, \quad (5)$$

$$I_{S,2} = \sum_{X_{S,i} \in \Phi_{S/X_{S,0}}} P_S g_{S,i} \left\| X_{S,i} \right\|^{-\alpha_s}. \quad (6)$$

1) Uplink/Downlink Information transmission:

During the UL-DL WIT phase, each MBS uses linear zero-forcing beamforming (ZFBF) with the equal transmit power allocation to transmit S data streams to associated DL UEs [9]. Therefore, the uncorrelated intra-cell interference is completely cancelled out. The signal-to-interference-plus-noise ratio (SINR) for a typical UE, located at the origin and associated with the MBS, can be written as

$$SINR_{U_0}^{dl,MBS} = \frac{\frac{P_M}{S} \beta \mathbf{h}_{M,0} \left\| X_{M,0} \right\|^{-\alpha_M}}{\underbrace{I_{M,i}^{dl} + I_{S,i}^{dl} + I_U^{dl}}_{I_M^{dl}} + \varepsilon P_{RSI}^U + N_0}, \quad (7)$$

where $\mathbf{h}_{M,0} \sim \text{Gamma}(N - S + 1)$ is the small-scale fading channel power gain between the typical DL UE and its serving MBS, and β is the frequency dependent constant value. $\varepsilon \in \{0,1\}$ is the SI factor: for FD UEs $\varepsilon = 1$ else $\varepsilon = 0$, $P_{RSI}^U = \text{E}\{P_{U_0}\} \left| h_{RSI}^U \right|^2$ is the residual SI power after performing SI cancellation, where $h_{RSI}^U \sim \exp(1)$ is the residual SI channel of the typical UEs [11]. Moreover, $I_{M,i}^{dl}$, $I_{S,i}^{dl}$, and I_U^{dl} are the interferences from the other MBSs, the SBSs, and the other FD UEs, respectively, given as

$$I_{M,i}^{dl} = \sum_{X_{M,i} \in \Phi_{M/X_{M,0}}} \frac{P_M}{S} \mathbf{h}_{M,i} \beta \left\| X_{M,i} \right\|^{-\alpha_M}, \quad (8)$$

$$I_{S,i}^{dl} = \sum_{X_{S,i} \in \Phi_S} P_S h_{S,i} \beta \left\| X_{S,i} \right\|^{-\alpha_s}, \quad (9)$$

and

$$I_U^{dl} = \sum_{X_{u_j} \in \Phi_{u/0}} \text{E}\{P_{U_j}\} g_{u_j} \beta \left\| X_{u_j} \right\|^{-\alpha_s}. \quad (10)$$

In (8), (9), and (10), $\mathbf{h}_{M,i} \sim \text{Gamma}(S,1)$, $h_{S,i} \sim \exp(1)$, and $g_{u_j} \sim \exp(1)$ denote the small-scale fading channel power gains from the interfering MBSs to the typical MCell DL UE, and from the SBSs to the typical MCell DL UE, and the FD UEs to the typical MCell DL UE, respectively, and their corresponding distances are denoted as $X_{M,i}$, $X_{S,i}$, and X_{u_j}, respectively. Finally, $\text{E}\{P_{U_j}\}$ denotes the transmit power of FD UEs which upload packets to SBSs.

Moreover, the SINR for a typical DL SCell UE located at the origin can be written as

$$SINR_{U_0}^{dl,SBS} = \frac{P_S \beta h_{S,0} \left\| X_{S,0} \right\|^{-\alpha_s}}{\underbrace{I_{M,i}^{dl} + I_{S,i}^{dl} + I_U^{dl}}_{I_S^{dl}} + \varepsilon P_{RSI}^U + N_0}, \quad (11)$$

where $h_{S,0} \sim \exp(1)$ and $\left\| X_{S,0} \right\|$ are the small-scale fading channel power gain and the distance between the typical DL SCell UE and its serving SBS and α_s is the path loss exponent for the SCell channel. Furthermore, $I_{M,i}^{dl}$, $I_{S,i}^{dl}$, and I_U^{dl} are the interference from the MBSs, the other SBSs, the other FD UEs, given as

$$I_{M,i}^{dl} = \sum_{X_{M,i} \in \Phi_M} \frac{P_M}{S} \mathbf{h}_{M,i} \beta \left\| X_{M,i} \right\|^{-\alpha_M}, \quad (12)$$

$$I_{S,i}^{dl} = \sum_{X_{S,i} \in \Phi_{S/X_{S,0}}} P_S h_{S,i} \beta \left\| X_{S,i} \right\|^{-\alpha_s}, \quad (13)$$

$$I_U^{dl} = \sum_{X_{u_j} \in \Phi_{u/0}} \text{E}\{P_{U_j}\} g_{u_j} \beta \left\| X_{u_j} \right\|^{-\alpha_s}. \quad (14)$$

In (12), (13), and (14) $\mathbf{h}_{M,i} \sim \text{Gamma}(S,1)$, $h_{S,i} \sim \exp(1)$, and $g_{u_j} \sim \exp(1)$ denote the small scale fading channel power gain to the DL SCell UE from the MBSs, the SBSs, the FD UEs, respectively, and their corresponding distances are denoted $X_{M,i}$, $X_{S,i}$, and, X_{u_j}, respectively. The UL SINR for a typical SBS located at the origin can be written as

$$SINR_{S,0}^{ul} = \frac{\text{E}\{P_{U_0}\} \beta g_{u_0} \left\| X_{u_0} \right\|^{-\alpha_s}}{\underbrace{I_{M,i}^{ul} + I_{S,i}^{ul} + I_U^{ul}}_{I_S^{ul}} + P_{RSI}^S + N_0}, \quad (15)$$

where $g_{u_0} \sim \exp(1)$ is the small-scale fading channel power gain between typical FD UE, and SBS $X_{S,i}$. $\left\| X_{u_0} \right\|$ is the distance between typical FD UE and its serving SBS and $P_{RSI}^S = P_S \left| h_{RSI}^S \right|^2$ is the residual SI power after performing cancellation, where $h_{RSI}^S \sim \exp(1)$ is the residual SI channel of the typical SBS [11]. Moreover $I_{M,i}^{ul}$, $I_{S,i}^{ul}$, and I_U^{ul} are the interference from the MBSs, the other SBSs, and the other FD UEs given as

$$I_{M,i}^{ul} = \sum_{X_{M,i} \in \Phi_M} \frac{P_M}{S} \mathbf{h}_{M,i} \beta \left\| X_{M,i} \right\|^{-\alpha_M}, \quad (16)$$

$$I_{S,i}^{ul} = \sum_{X_{S,i} \in \Phi_{S/0}} P_S h_{S,i} \beta \left\| X_{S,i} \right\|^{-\alpha_s}, \quad (17)$$

$$I_U^{ul} = \sum_{X_{u_j} \in \Phi_{u/0}} \text{E}\{P_{U_j}\} g_{u_j} \beta \left\| X_{u_j} \right\|^{-\alpha_s}. \quad (18)$$

In (16), (17), and (18) $\mathbf{h}_{M,i} \sim \text{Gamma}(S,1)$, $h_{S,i} \sim \exp(1)$, and $g_{u_j} \sim \exp(1)$ denote the small scale fading channel power gain to the SBS from the MBSs, the SBSs, the FD UEs, respectively, and their corresponding distances are denoted as $X_{M,i}$, $X_{S,i}$, and X_{u_j}, respectively.

III. Performance Analysis

In this section, we provide the performance analysis of the proposed DUDe user association scheme in terms of the average UL power transfer and coverage probability analysis. We further characterize the ASE and EE of the proposed scheme. Some key preliminary results are given first for the DL and UL user association probability as well as the probability density function (pdf) of the distance between a typical UE and its serving BS, for the proposed DUDs user association scheme.

A. Preliminary Results

1) DL user association probability and pdf of the distance between typical UE and serving MBS:

Lemma 1: The probability that a typical UE is associated with the MBS based on MMPA scheme is given by

$$\Lambda_M = 2\pi\lambda_M \int_0^{\infty} r \exp\left(-\pi\lambda_M r^2 - \pi\lambda_S \left(\frac{SP_S}{P_M}\right)^{\frac{2}{\alpha_s}} r^{\frac{2\alpha_M}{\alpha_s}} \right) dr. \quad (19)$$

Proof: See Appendix A. ■

Lemma 2: The pdf of the distance between a typical UE and its serving MBS given by

$$f_{X_{M,i}}(x) = \frac{2\pi\lambda_M}{\Lambda_M} x \exp\left(-\pi\lambda_M x^2 - \pi\lambda_s \left(\frac{SP_S}{P_M}\right)^{\frac{2}{\alpha_s}} x^{\frac{2\alpha_M}{\alpha_s}} \right). \quad (20)$$

Proof: See Appendix B. ■

Lemma 3: The probability that a typical UE is associated with the SBS based on MMPA scheme is given by

$$\Lambda_{S^{dl}} = 2\pi\lambda_S \int_0^{\infty} r \exp\left(-\pi\lambda_M \left(\frac{P_M}{SP_S}\right)^{\frac{2}{\alpha_M}} r^{\frac{2\alpha_s}{\alpha_M}} - \pi\lambda_S r^2 \right) dr. \quad (21)$$

Proof: The proof is similar to the proof of Lemma 1 and thus omitted. ■

Lemma 4: The pdf of the distance between a typical UE and its serving SBS given by

$$f_{X_{S,i}}(x) = \frac{2\pi\lambda_S}{\Lambda_{S^{dl}}} x \exp\left(-\pi\lambda_M \left(\frac{P_M}{SP_S}\right)^{\frac{2}{\alpha_M}} x^{\frac{2\alpha_s}{\alpha_M}} - \pi\lambda_S x^2 \right). \quad (22)$$

Proof: The proof is similar to the proof of Lemma 2 and thus omitted. ■

2) UL user association and pdf of the distance between typical UE and serving SBS:

A typical FD UE in UL transmission can only be associated with FD SBSs independent of the DL serving BSs (i.e. A typical FD UE associate with BS (MBS/SBS) b in DL and different BS (SBS) b′ in UL).

Lemma 5: The pdf of the distance between a typical UE and associated SBS given by

$$f_{X_{S,i}}^{NBA}(x) = 2\pi\lambda_S x \exp\left(-\pi\lambda_S x^2\right). \quad (23)$$

B. Analysis Of Average Uplink Power Transfer

To ascertain the UL transmit power of a typical UE in the *mth* tier, $m \in \{M, S\}$, we characterize the average received power at the typical UE with the MMPA scheme in the following Theorems.

Theorem 1: For the MMPA scheme, the average received power at the typical UE associated with the MBS, is given by

$$\mathrm{E}\left\{P_{U_j}\right\}\Big|_{MBS} = \mu 2\pi\lambda_M \left(P_M \left(\kappa\Xi_1 + \frac{2\pi\lambda_M}{\alpha_M - 2}\Xi_2 \right) + \frac{2\pi\lambda_S}{\alpha_s - 2}\Xi_3 P_S \right), \quad (24)$$

where $\kappa = \frac{N+S-1}{S}$,

$$\Xi_1 = \int_0^{\infty} \frac{x^{1-\alpha_M}}{\Lambda_M} \exp\left(-\pi\lambda_s \left(\frac{SP_S}{P_M}\right)^{\frac{2}{\alpha_s}} x^{\frac{2\alpha_M}{\alpha_s}} - \pi\lambda_M x^2 \right) dx, \quad (25a)$$

$$\Xi_2 = \int_0^{\infty} \frac{x^{3-\alpha_M}}{\Lambda_M} \exp\left(-\pi\lambda_s \left(\frac{SP_S}{P_M}\right)^{\frac{2}{\alpha_s}} x^{\frac{2\alpha_M}{\alpha_s}} - \pi\lambda_M x^2 \right) dx, \quad (25b)$$

$$\Xi_3 = \int_0^{\infty} \frac{x\,\rho_s(x)^{2-\alpha_s}}{\Lambda_{S^{dl}}} \exp\left(-\pi\lambda_s \left(\frac{SP_S}{P_M}\right)^{\frac{2}{\alpha_s}} x^{\frac{2\alpha_M}{\alpha_s}} - \pi\lambda_M x^2 \right) dx, \quad (25c)$$

and $\rho_S(x) = \left(\frac{SP_S}{P_M}\right)^{\frac{1}{\alpha_s}} x^{\frac{\alpha_M}{\alpha_s}}$ is the distance between the closest interfering SBS of the second tier and the typical MCell UE.

Proof: The proof is straightforward and thus omitted. ■

Theorem 2: The average received power at the typical UE associated with the SBS based on MMPA scheme is given by

$$\mathrm{E}\left\{P_{U_j}\right\}\Big|_{SBS} = \mu 2\pi\lambda_S \left(P_S \left(\varpi_1 + \frac{2\pi\lambda_S}{\alpha_s - 2}\varpi_2 \right) + \frac{2\pi\lambda_M}{\alpha_M - 2} P_M \varpi_3 \right), \quad (26)$$

where

$$\varpi_1 = \int_0^{\infty} \frac{x^{1-\alpha_s}}{\Lambda_{S^{dl}}} \exp\left(-\pi\lambda_M \left(\frac{P_M}{SP_S}\right)^{\frac{2}{\alpha_M}} x^{\frac{2\alpha_s}{\alpha_M}} - \pi\lambda_s x^2 \right) dx, \quad (27a)$$

$$\varpi_2 = \int_0^{\infty} \frac{x^{3-\alpha_s}}{\Lambda_{S^{dl}}} \exp\left(-\pi\lambda_M \left(\frac{P_M SP_S}{SP_S}\right)^{\frac{2}{\alpha_M}} x^{\frac{2\alpha_s}{\alpha_M}} - \pi\lambda_s x^2 \right) dx, \quad (27b)$$

$$\varpi_3 = \int_0^{\infty} \frac{x\,\rho_M(x)^{2-\alpha_M}}{\Lambda_M} \exp\left(-\pi\lambda_M \left(\frac{P_M SP_S}{SP_S}\right)^{\frac{2}{\alpha_M}} x^{\frac{2\alpha_s}{\alpha_M}} - \pi\lambda_s x^2 \right) dx, \quad (27c)$$

where $\rho_M = \left(\frac{P_M}{SP_S}\right)^{\frac{1}{\alpha_M}} x^{\frac{\alpha_s}{\alpha_M}}$ is the distance between the closest interfering MBS and the typical SCell UE [26].

Proof: The proof is straightforward and thus omitted. ■

C. Coverage Probability

In this section, we study the coverage probability of two-tier HetNet with FD SCell.

1) Downlink analysis: Since the typical UE can only be associated with one tier, from the law of total probability, the DL coverage probability [9] is given by

$$C^{DL}\left(R^{DL}\right) = \sum_{m\in\{M,S\}} \Lambda_m C_m^{DL}\left(R^{DL}\right), \tag{28}$$

where Λ_m is the per-tier association probability, C_m^{DL} is the coverage probability of a typical UE associated with mth tier BSs, and R^{DL} is the DL rate threshold. For a SINR threshold γ_{th}^{dl} and a typical UE $SINR_m$ at a distance x from its associated BS, the coverage probability is given by

$$C_m^{DL}\left(R^{DL}\right) = \mathrm{E}_X\left\{\Pr\left(SINR_m(x) \geq \gamma_{th}^{dl} \middle| x\right)\right\}, \tag{29}$$

where $\gamma_{th}^{dl} = 2^{R^{DL}} - 1$.

Theorem 3: The DL coverage probability of a typical UE associated with the MBS based on MMPA scheme is derived as

$$C_M\left(R^{DL}\right) = \frac{2\pi\lambda_M}{\Lambda_M}\int_0^\infty x\left[\frac{1}{2}\left(\exp\left(-\pi\lambda_M x^2 - \pi\lambda_S\left(\frac{SP_S}{P_M}\right)^{\frac{2}{\alpha_s}} x^{\frac{2\alpha_M}{\alpha_s}}\right)\right)\right.$$
$$-\frac{1}{\pi}\int_0^\infty \mathrm{Im}\left[\exp\left(-\Omega_1(x,\omega) - \pi\lambda_M\Omega_2(x,\omega) - 2\pi\lambda_S\right.\right.$$
$$\left.\left.\left(\Omega_3(x,\omega)+\Omega_4(x,\omega)\right) - \pi\lambda_M x^2 - \pi\lambda_S\left(\frac{SP_S}{P_M}\right)^{\frac{2}{\alpha_s}} x^{\frac{2\alpha_M}{\alpha_s}}\right)\right.$$
$$\left.\left(1+\varepsilon(-j\omega)\mathrm{E}\left\{P_{U_0}\right\}\right)^{-1}\right]\frac{d\omega}{\omega}\left.\right]dx, \tag{30}$$

where

$$\Omega_1(x,\omega) = j\omega\left(\frac{\beta P_M}{\gamma_{mM}^{dl} x^{\alpha_M}} - N_0\right), \tag{31a}$$

$$\Omega_2(x,\omega) = \frac{\Gamma\left(1-\frac{2}{\alpha_M}\right) + \frac{2}{\alpha_M}\Gamma_u\left(-\frac{2}{\alpha_M}, \frac{-j\omega\beta P_M}{x^{\alpha_M}}\right)}{\left(-j\omega\beta P_M\right)^{\frac{2}{\alpha_M}}} - x^2, \tag{31b}$$

$$\Omega_3(x,\omega) = \frac{(-j\omega)\beta P_S^{\frac{2}{\alpha_s}}\left(\frac{Sx^{\alpha_M}}{P_M}\right)^{\frac{2}{\alpha_s}-1}}{\alpha_s - 2} \times {}_2F_1\left[1, 1-\frac{2}{\alpha_s}; 2-\frac{2}{\alpha_s}; \frac{(j\omega)\beta P_M}{Sx^{\alpha_M}}\right], \tag{31c}$$

$$\Omega_4(x,\omega) = \frac{1}{2}\Gamma\left(1+\frac{2}{\alpha_s}\right)\Gamma\left(1-\frac{2}{\alpha_s}\right)\left(\Lambda_M(-j\omega \times \mathrm{E}\left\{P_{U_0}\right\}\Big|_{MBS}) + \Lambda_{S^{dl}}\left(-j\omega\mathrm{E}\left\{P_{U_0}\right\}\Big|_{SBS}\right)\right), \tag{31d}$$

and $\gamma_{mM}^{dl} = \frac{\gamma_{th}^{dl}}{\Upsilon}$, $\mathrm{E}\left\{P_{U_j}\right\}\Big|_{MBS}$ and $\mathrm{E}\left\{P_{U_j}\right\}\Big|_{SBS}$ are given in (24) and (26), respectively.

Proof: See Appendix C. ■

Theorem 4: The DL coverage probability of a typical UE associated with the SBS based on MMPA user association scheme is derived as

$$C_{S^{dl}}\left(R^{DL}\right) = \frac{2\pi\lambda_S}{\Lambda_{S^{dl}}}\int_0^\infty x\left[\frac{1}{2}\left(\exp\left(-\pi\lambda_M\left(\frac{P_M}{SP_S}\right)^{\frac{2}{\alpha_M}} x^{\frac{2\alpha_s}{\alpha_M}} - \pi\lambda_S x^2\right)\right)\right.$$
$$-\frac{1}{\pi}\int_0^\infty \mathrm{Im}\left[\exp\left(j\omega N_0 - \pi\lambda_M\Theta_1(x,\omega) - 2\pi\lambda_S\right.\right.$$
$$\left.\left.\left(\Theta_2(x,\omega)+\Theta_3(x,\omega)\right) - \pi\lambda_M\left(\frac{P_M}{SP_S}\right)^{\frac{2}{\alpha_M}} x^{\frac{2\alpha_s}{\alpha_M}} - \pi\lambda_S x^2\right)\right.$$
$$\left.\left(1+\frac{j\omega\beta P_S}{\gamma_{th}^{dl} x^{\alpha_s}}\right)^{-1}\left(1+\varepsilon(-j\omega)\mathrm{E}\left\{P_{U_0}\right\}\right)^{-1}\right]\frac{d\omega}{\omega}\left.\right]dx, \tag{32}$$

where

$$\Theta_1(x,\omega) = \frac{\Gamma\left(1-\frac{2}{\alpha_M}\right) + \frac{2}{\alpha_M}\Gamma_u\left(-\frac{2}{\alpha_M}, \frac{-j\omega\beta P_M}{(\rho_M)^{\alpha_M}}\right)}{\left(-j\omega\beta P_M\right)^{\frac{2}{\alpha_M}}} - \left(\rho_M(x)\right)^2, \tag{33a}$$

$$\Theta_2(x,\omega) = \frac{(-j\omega)\beta P_S x^{2-\alpha_s}}{\alpha_s - 2} \times {}_2F_1\left[1, 1-\frac{2}{\alpha_s}; 2-\frac{2}{\alpha_s}; \frac{(j\omega)\beta P_S}{x^{\alpha_s}}\right], \tag{33b}$$

$$\Theta_3(x,\omega) = \frac{1}{2}\Gamma\left(1+\frac{2}{\alpha_s}\right)\Gamma\left(1-\frac{2}{\alpha_s}\right)\left(\Lambda_M(-j\omega \times \mathrm{E}\left\{P_{U_0}\right\}\Big|_{MBS}) + \Lambda_{S^{dl}}\left(-j\omega\mathrm{E}\left\{P_{U_0}\right\}\Big|_{SBS}\right)\right), \tag{33c}$$

Proof: The proof is similar to that of Theorem 3 and thus omitted. ■

2) Uplink analysis: The coverage probability that a typical UE is associated with SBS $C_S^{UL}\left(R^{UL}\right)$ is defined as

$$C_S^{UL}\left(R^{UL}\right) = \mathrm{E}_{\|X_{U_0}\|}\left\{\Pr\left[SINR_{S,0}^{ul}\left(\|X_{U_0}\|\right) \geq \gamma_{th}^{ul} \middle| \|X_{U_0}\|\right]\right\}, \tag{34}$$

where $SINR_{S,0}^{ul}$ is given in (15), $\gamma_{th}^{ul} = 2^{R^{UL}} - 1$ and R^{UL} is the UL rate threshold.

Theorem 5: The UL coverage probability of a typical UE associated with SBS based on NBA scheme is given by

$$C_S^{UL}\left(R^{UL}\right)=$$
$$2\pi\lambda_S\int_0^{\infty}x\left[\frac{1}{2}\left(\exp\left(-\pi\lambda_S x^2\right)\right)-\frac{1}{\pi}\int_0^{\infty}\mathrm{Im}\left[\exp\left(j\omega N_0\right)\right.\right.$$
$$\left.-\pi\lambda_M\,\xi_1(x,\omega)-2\pi\lambda_S\left(\xi_2(x,\omega)+\xi_3(x,\omega)\right)-\pi\lambda_S x^2\right)$$
$$\left(1+\frac{j\omega\beta\,\mathrm{E}\left\{P_{U_j}\right\}}{\gamma_{th}^{ul}\,x^{\alpha_s}}\right)^{-1}\left(1+\varepsilon(-j\omega)P_S\right)^{-1}\Big]\frac{d\omega}{\omega}\Big]dx, \quad (35)$$

where

$$\xi_1(x,\omega)=\frac{\Gamma\left(1-\frac{2}{\alpha_M}\right)+\frac{2}{\alpha_M}\Gamma_u\left(-\frac{2}{\alpha_M},\frac{-j\omega\beta P_M}{R^{\alpha_M}}\right)}{\left(-j\omega\beta P_M\right)^{\frac{2}{\alpha_M}}}-R^2, \quad (36a)$$

$$\xi_2(x,\omega)=\frac{(-j\omega)\beta P_S R^{2-\alpha_s}}{\alpha_s-2}$$
$$\times\,{}_2F_1\left[1,1-\frac{2}{\alpha_s};2-\frac{2}{\alpha_s};\frac{(j\omega)\beta P_S}{R^{\alpha_s}}\right], \quad (36b)$$

$$\xi_3(x,\omega)=\frac{1}{2}\Gamma\left(1+\frac{2}{\alpha_s}\right)\Gamma\left(1-\frac{2}{\alpha_s}\right)\left(\Lambda_M\left(-j\omega\right.\right.$$
$$\left.\left.\times\mathrm{E}\left\{P_{U_0}\right\}\Big|_{MBS}\right)+\Lambda_{S^{dl}}\left(-j\omega\mathrm{E}\left\{P_{U_0}\right\}\Big|_{SBS}\right)\right). \quad (36c)$$

D. Area Spectral Efficiency And Energy Efficiency

In this subsection, we consider ASE, that describe the sum throughput for all UE per unit area. Furthermore, we evaluate the EE of the considered FD HetNet, which is one of the important design parameters in 5G systems. The EE is defined as the ratio of the SE to the average power consumption [27].

The DL ASE of the typical UE associated to MBS can be obtained as

$$ASE_M=\lambda_M S\,C_M\left(R^{DL}\right)\ln\left(1+\gamma_{mM}^{dl}\right), \quad (37)$$

where $C_M\left(R^{DL}\right)$ is given in (30). Moreover, the DL ASE of the typical UE associated to the SBS is given by

$$ASE_{S^{dl}}=\lambda_S C_{S^{dl}}\left(R^{DL}\right)\ln\left(1+\gamma_{th}^{dl}\right), \quad (38)$$

where $C_{S^{dl}}\left(R^{DL}\right)$ is given in (33).

The ASE of the typical user in UL associated to the SBS is given by

$$ASE_{S^{ul}}=\lambda_S C_{S^{ul}}\left(R^{UL}\right)\ln\left(1+\gamma_{th}^{ul}\right), \quad (39)$$

where $C_{S^{ul}}\left(R^{UL}\right)$ is given in (36).

The EE for a typical UL UE is given by

$$EE_u=\frac{ASE_{S^{ul}}}{\mathrm{E}\left\{P_u\right\}^{total}}, \quad (40)$$

where $ASE_{S^{ul}}$ is the UL ASE is given in (39), and the average total power can be derived as

$$\mathrm{E}\left\{P_u\right\}^{total}=P_f+\frac{\mathrm{E}\left\{P_U\right\}}{\rho}, \quad (41)$$

where

$$\mathrm{E}\left\{P_U\right\}=\lambda_S\left(\Lambda_M\,\mathrm{E}\left\{P_U\right\}\Big|^{MBS}+\Lambda_{S^{dl}}\,\mathrm{E}\left\{P_U\right\}\Big|^{SBS}\right), \quad (42)$$

while P_f is the fixed circuit power use, $\mathrm{E}\left\{P_U\right\}\Big|^{MBS}$ and $\mathrm{E}\left\{P_U\right\}\Big|^{SBS}$ are the average transmit power given by (24) and (26), respectively. For UL transmission, the average transmit power of a UE depends on which BSs the UE is associated with during the DL-WPT phase and, ρ is the power amplifier efficiency.

IV. Numerical Results and Discussion

In this section, we evaluate the performance of the proposed DUDe user association scheme for the wireless-powered FD HetNet. Monte Carlo simulations are conducted to validate the accuracy of the theoretical framework. We assume that the BSs and UEs are distributed randomly within the circle area with radius r. Table I reports a list of the parameter values used in this section.

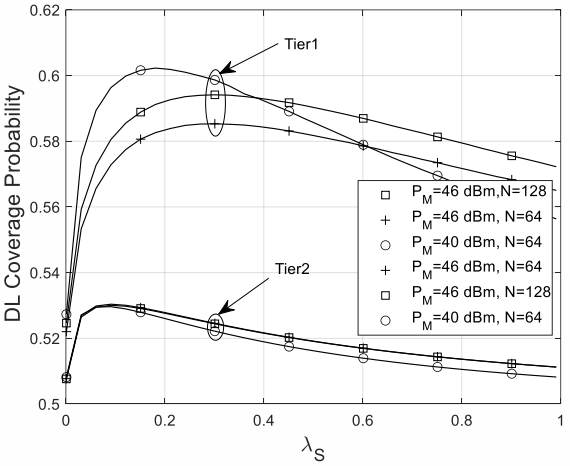

Fig. 2. DL coverage probability vs. the density of SBSs (λ_S), $S=15$.

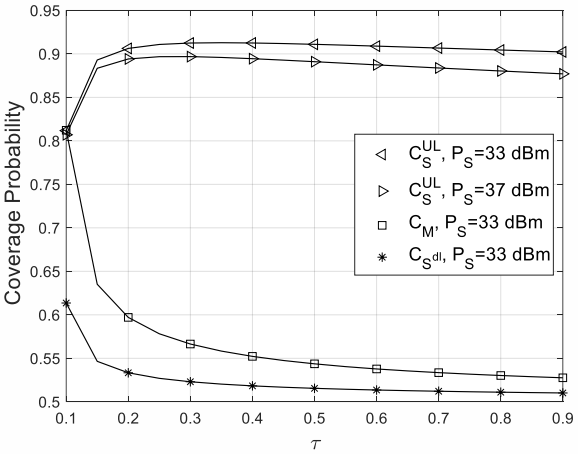

Fig. 3. DL and UL coverage probability versus τ ($P_M=40$dBm, $S=15$, $\lambda_S=0.2$).

TABLE I. SYSTEM PARAMETER'S.

Parameter	Value	Parameter	Value
P_M	40 dBm	P_S	33 dBm
α_M	3.5	α_s	4
β	0.9	η	0.9
S	5	N_0	-100 dBm
P_f	0.1 W	ρ	5
R^{DL}	0.5	R^{UL}	0.5

Fig. 2 shows the DL coverage probability C_M and $C_{S^{dl}}$, versus λ_S for two different values of P_M, N, and S. Analytical results have been included from (30) and (32). It is clear that the simulation results (markers) are in exact agreement with the theoretical results (solid lines). By increasing λ_S the DL coverage probability at both tiers improves at first, which is due to the fact that increasing λ_S reduced the link distance between the typical UE and its serving SBS. Therefore, most UEs preferring to associate with SBS than the MBSs. However, increasing λ_S reduces coverage probability to some extent since it increases received interference from SBSs, as well as interference from

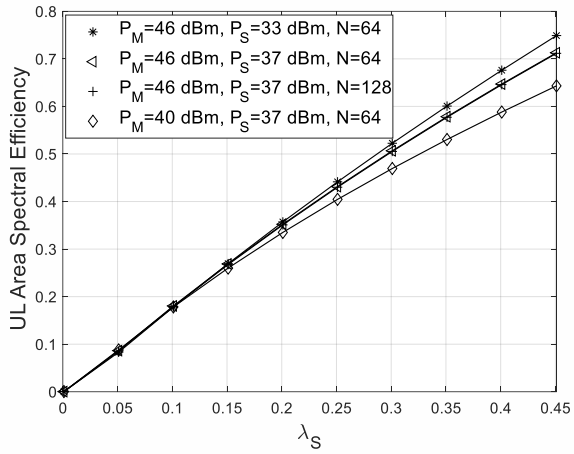

(a)

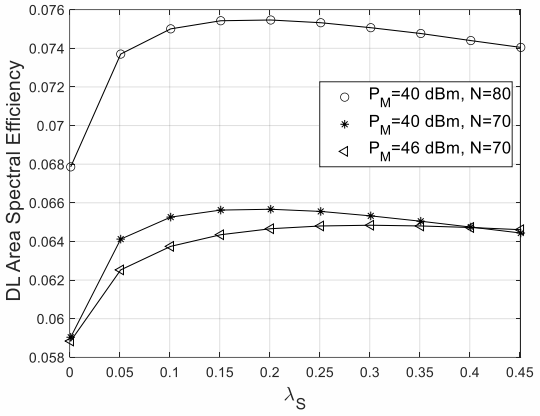

(b)

Fig. 4. (a) UL area spectral efficiency vs. the density of SBSs (λ_S) ($S = 5$). And (b) DL area spectral efficiency vs. the density of SBSs (λ_S) ($S = 5$).

UEs transmitting in UL. Moreover, the increase in N improves the DL MBS coverage probability. This can be explained by the fact when N increases the MBS power gain is boosted. On the other hand, DL SBS coverage probability decrease by increasing N. This can be explained by the fact when N increases the MBS power gain is boosted. On the other hand, DL SBS coverage probability decrease by increasing N. This is because when N increase the amount of the harvested power from MBS is increased, which accordingly increases interference from other MBSs and UL UEs. Finally, we observe that as P_M increases in both tiers, the probability of DL coverage increases at higher values of λ_S.

Fig. 3 compares the UL and DL coverage probability of the typical UEs τ (i.e., WPT duration) is increased. By increasing τ DL coverage probability for both tiers reduces, while the UL coverage probability increases. This can be explained by the fact that harvested power increases when τ increased. Therefore, the interference caused by the UL transmissions of FD UEs increases which in turn reduces the DL coverage probability. It is evident that,

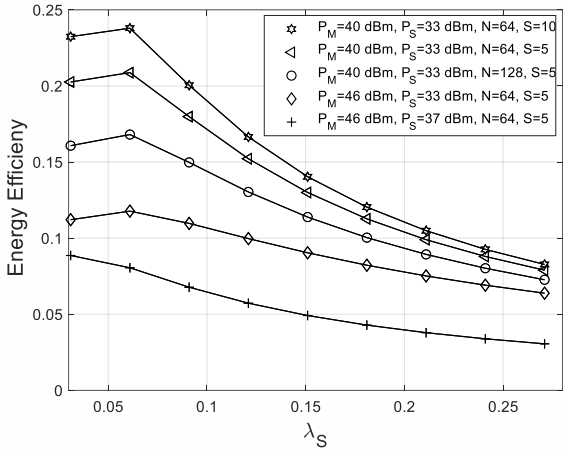

Fig. 5. Energy efficiency in UL link vs. the density of SBSs (λ_S) ($S = 5$).

when P_S increases, the UL coverage probability decreases due to increase of the SI.

Fig. 4 represents the DL and UL ASE. In Fig 4a. we investigate the UL ASE, defined in (39), versus λ_S for two values of P_M, P_S, and N. It is clear that as expected the UL ASE increases when λ_S increases. This is due to the fact that UEs become closed to the SBSs and thus the link distances are shortened which in turn improves the EH efficiency. Moreover, the more number of UEs can be served through the SBSs. Therefore, the more number of UEs with more level of transmit power can be served in the UL. Furthermore, the UL ASE reduces when P_S increased due to increase of the SI strength. In Fig 4b. the DL ASE for

MCell, defined in (37), is plotted versus λ_S. We can observe that DL ASE shows the same trend as the DL coverage probability, i.e., increase for small values of λ_S and then starts to decrease. The DL ASE improves when the MBS transmit power increased due to improvement of the received power. Moreover, the DL ASE increases when N increased which is due to the fact the MBS transmit power increases.

Fig. 5 shows the EE of the UL transmission, defined in (40), versus λ_S and for two values of P_M, P_S, and N. By increasing λ_S the EE in UL decreases, which is due to the fact that increasing λ_S increased the UE power consumption as the harvested power at UE increases. Moreover, by increasing N the UL EE decreases. This can be explained by the fact when N becomes larger the harvested power at each UE is boosted that cause an increase in the UE power consumption.

V. Conclusion

In this paper, we presented an analytical framework to study the performance of DUDe user association in the FD wireless-powered two-tier HetNets. We proposed DL MMPA and the UL NBA user association schemes and derived closed-form expressions of the UL and DL coverage probabilities, ASE as well as UL EE. Our analysis provides an efficient means of evaluating the impact of the MBS density, SBS density, and corresponding transmit powers on the UL and DL coverage, as well as EE of the considered system. Numerical results shown that when the SBS density increases, the UL EE decreases while the UL and DL coverage probabilities and ASE increase. Thus, for different system configurations, there is an optimum value for the SBS density at which both the DL and UL coverage probabilities are maximized, and ASE and EE provide optimum performances.

Appendix A

Proof of Lemma 1

A typical UE is associated with MBS based on MMPA scheme in DL when $\frac{P_M}{S}\|X_{M,0}\|^{-\alpha_M} > P_S\|X_{S,0}\|^{-\alpha_S}$. Therefore,

$$\begin{aligned}\Lambda_M &= \mathrm{E}_{X_M}\left\{\Pr\left(P_{x,M} \succ P_{x,S}\right)\right\}\\ &= \mathrm{E}_{X_M}\left\{\Pr\left(P_{x,M}\left(X_{M,0}\right) \succ P_{x,S}\left(X_{S,0}\right)\right)\right\}\\ &= \mathrm{E}_{X_M}\left\{\Pr\left(\frac{P_M}{S}\|X_{M,0}\|^{-\alpha_M} \succ P_S\|X_{S,0}\|^{-\alpha_S}\right)\right\}\\ &= \mathrm{E}_{X_M}\left\{\Pr\left(\|X_{S,0}\| \succ \left(\frac{SP_S}{P_M}\right)^{\frac{1}{\alpha_S}}\|X_{M,0}\|^{\frac{\alpha_M}{\alpha_S}}\right)\right\}\\ &= \int_0^\infty \Pr\left(\|X_{S,0}\| \succ \left(\frac{SP_S}{P_M}\right)^{\frac{1}{\alpha_S}}\|X_{M,0}\|^{\frac{\alpha_M}{\alpha_S}}\right) f_{X_M}(x)\,dx,\end{aligned} \tag{43}$$

where $\Pr\left(\|X_{S,0}\| > \left(\frac{SP_S}{P_M}\right)^{\frac{1}{\alpha_S}}\|X_{M,0}\|^{\frac{\alpha_M}{\alpha_S}}\right)$ and pdf of the $X_{M,0}$ are derived using the null probability of a $2-D$ Poisson point process with density λ in an area A, which is $\exp(-\lambda A)$. Therefore, we have

$$\begin{aligned}&\Pr\left(\|X_{S,0}\| \succ \left(\frac{SP_S}{P_M}\right)^{\frac{1}{\alpha_S}}\|X_{M,0}\|^{\frac{\alpha_M}{\alpha_S}}\right)\\ &= \exp\left(-\pi\lambda_S\left(\frac{SP_S}{P_M}\right)^{\frac{1}{\alpha_S}}\|X_{M,0}\|^{\frac{\alpha_M}{\alpha_S}}\right).\end{aligned} \tag{44}$$

And

$$\begin{aligned}f_{X_M}(x) &= 1-\frac{d}{dx}\left(\Pr\left(X_{M,0} \succ x\right)\right)\\ &= 2\pi\lambda_M x\exp\left(-\pi\lambda_M x^2\right).\end{aligned} \tag{45}$$

Finally, by substituting (45) and (44) into (43) we obtain (19).

Appendix B

Proof of Lemma 2

When the typical UE is associated with MBS, probability of $X_{M,0} > x$ can be obtained as

$$\begin{aligned}\Pr\left(X_{M,0} \succ x\right) &= \Pr\left(X_{M,0} \succ x \,|\, n = M\right)\\ &= \frac{\Pr\left(X_{M,0} \succ x, n = M\right)}{\Pr\left(n = M\right)},\end{aligned} \tag{46}$$

where $\Pr(n = M) = \Lambda_M$ given in (19), and the joint probability of $X_{M,0} > x$ and $n = M$ is

$$\begin{aligned}&\Pr\left(X_{M,0} \succ x, n = M\right) =\\ &\Pr\left(X_{M,0} \succ x, P_{x,M}\left(X_{M,0}\right) \succ P_{x,S}\left(X_{S,0}\right)\right)\\ &= \int_x^\infty \Pr\left(\|X_{S,0}\| \succ \left(\frac{SP_S}{P_M}\right)^{\frac{1}{\alpha_S}}\|X_{M,0}\|^{\frac{\alpha_M}{\alpha_S}}\right) f_{X_M}(x)\,dx\end{aligned}$$

$$= 2\pi\lambda_M \int_x^{\infty} x \exp\left(-\pi\lambda_M x^2 - \pi\lambda_s \left(\frac{SP_S}{P_M}\right)^{\frac{2}{\alpha_s}} x^{\frac{2\alpha_M}{\alpha_s}}\right) dx. \quad (47)$$

By substituting (47) into (46) we get

$$\Pr\left(X_{M,0} \succ x\right) = \frac{2\pi\lambda_M}{\Lambda_M^{MMPA}} \int_x^{\infty} x \exp\left(-\pi\lambda_M x^2 - \pi\lambda_s \left(\frac{SP_S}{P_M}\right)^{\frac{2}{\alpha_s}} x^{\frac{2\alpha_M}{\alpha_s}}\right) dx. \quad (48)$$

The cumulative distribution function (cdf) of $X_{M,0}$ is $F_{X_{M,0}}(x) = 1 - \Pr\left(X_{M,0} > x\right)$ and the pdf is given as

$$f_{X_{M,0}}(x) = \frac{dF_{X_{M,0}}(x)}{dx}. \quad (49)$$

By substituting (48) into (49), after some algebraic manipulations, the desired result in (20) is obtained.

Appendix C

Proof of Theorem 3

From (29) the DL coverage probability for MCell assuming $\|X_{M,0}\| = x$ is defined as

$$C_M\left(R^{DL}\right) = \mathrm{E}_{\|X_{M,0}\|}\left\{\mathrm{E}_{SINR_{U_0}^{dl,MBS}}\left\{\Pr\left(SINR_{U_0}^{dl,MBS}(x) \geq \gamma_{th}^{dl} \middle| x\right)\right\}\right\}, \quad (50)$$

where $SINR_{U_0}^{dl,MBS}$ from (7). Then with deconditioning over $\|X_{M,0}\|$ the coverage probability is given by

$$\begin{aligned} C_M &= \int_0^{\infty} \Pr\left(SINR_{U_0}^{dl,MBS} \geq \gamma_{th}^{dl} \middle| \|X_{M,0}\|\right) f_{\|X_{M,0}\|}(x)dx \\ &= \int_0^{\infty} \Pr\left(\frac{\frac{P_M}{S}\beta \mathbf{h}_{M,0}\|X_{M,0}\|^{-\alpha_M}}{\underbrace{I_{M,i}^{dl} + I_{S,i}^{dl} + I_U^{dl}}_{I_M^{dl}} + \varepsilon P_{RSI}^U + N_0} \geq \gamma_{th}^{dl}\right) f_{\|X_{M,0}\|}(x)dx \\ &\overset{(a)}{=} \int_0^{\infty} \Pr\left(\frac{P_M\beta\|X_{M,0}\|^{-\alpha_M}}{I_M^{dl} + \varepsilon P_{RSI}^U + N_0} \geq \gamma_{mM}^{dl}\right) f_{\|X_{M,0}\|}(x)dx \\ &= \int_0^{\infty} \Pr\left(I_M^{dl} \leq \frac{P_M\beta}{\gamma_{mM}^{dl}\|X_{M,0}\|^{\alpha_M}} - \varepsilon P_{RSI}^U - N_0\right) f_{\|X_{M,0}\|}(x)dx \\ &\overset{(b)}{=} \int_0^{\infty} F_{I_M^{dl}|_{mM}}\left(\frac{P_M\beta}{\gamma_{mM}^{dl}\|X_{M,0}\|^{\alpha_M}} - \varepsilon P_{RSI}^U - N_0\right) f_{\|X_{M,0}\|}(x)dx, \end{aligned} \quad (51)$$

where $f_{\|X_{M,0}\|}(x)$ from (20), (a) follows from $\mathbf{h}_{M,0} \sim \mathrm{Gamma}(N - S + 1)$, and (b) applied the Gil-Pelaez inversion theorem [9]. Furthermore, the cdf of the interference $F_{I_M^{dl}|_{mM}}(\cdot)$ can be derived as

$$F_{I_M^{dl}|_{mM}}(x) = \frac{1}{2} - \frac{1}{\pi} \times \int_0^{\infty} \mathrm{Im}\left[\frac{L_{I_M^{dl}}(-j\omega)}{\exp\left(j\omega\left(\frac{P_M\beta}{\gamma_{mM}^{dl}\|X_{M,0}\|^{\alpha_M}} - \varepsilon P_{RSI}^U - N_0\right)\right)}\right]\frac{d\omega}{\omega}, \quad (52)$$

where $\mathrm{Im}(\cdot)$ is the imaginary part of the argument. In (52), $L_{I_M^{dl}}(-j\omega)$ is the Laplace transform pdf of I_M^{dl} given as

$$L_{I_M^{dl}}(-j\omega) = L_{I_{M,i}^{dl}}(-j\omega) \times L_{I_{S,i}^{dl}}(-j\omega) \times L_{I_U^{dl}}(-j\omega), \quad (53)$$

where $L_{I_{M,i}^{dl}}(-j\omega)$, $L_{I_{S,i}^{dl}}(-j\omega)$, and $L_{I_U^{dl}}(-j\omega)$ are the Laplace transform of the pdf of $I_{M,i}^{dl}$, $I_{S,i}^{dl}$, and I_U^{dl}, respectively. In (53), $L_{I_{M,i}^{dl}}(-j\omega)$ calculated as

$$\begin{aligned} &L_{I_{M,i}}(-j\omega) \\ &= \mathrm{E}\left\{e^{-(-j\omega)I_{M,i}}\right\} = \mathrm{E}\left\{e^{-(-j\omega)\sum_{X_{M,i}\in\Phi_{M/X_{M,0}}} P_M\beta\|X_{M,i}\|^{-\alpha_M}}\right\} \\ &= \mathrm{E}_{\Phi}\left\{\exp\left(-(-j\omega)\sum_{X_{M,i}\in\Phi_{M/X_{M,0}}} P_M\beta\|X_{M,i}\|^{-\alpha_M}\right)\right\} \\ &= \mathrm{E}_{\Phi}\left\{\prod_{X_{M,i}\in\Phi_{M/X_{M,0}}} \exp\left(-(-j\omega)P_M\beta\|X_{M,i}\|^{-\alpha_M}\right)\right\} \\ &\overset{(a)}{=} \exp\left(-2\pi\lambda_M\int_x^{\infty}\left(1-\exp\left(-(-j\omega)P_M\beta x^{-\alpha_M}\right)\right)xdx\right), \end{aligned} \quad (54)$$

where is obtained by using probability generating functional (PGFL) of PPP, and x is the shortest distance between typical UE and interfering MBS. Likewise, the $L_{I_{S,i}^{dl}}(-j\omega)$ is evaluated as

$$\begin{aligned} &L_{I_{S,i}}(-j\omega) \\ &= \exp\left(-2\pi\lambda_S\int_{\rho_S(x)}^{\infty}\left(1-\mathrm{E}_h\left\{\exp\left(-(-j\omega)P_S\beta h_{S,i}\|X_{S,i}\|^{-\alpha_s}\right)\right\}\right)xdx\right), \\ &\overset{(a)}{=} \exp\left(-2\pi\lambda_S\int_{\rho_S(x)}^{\infty}\left(\frac{1}{1+\left((-j\omega)P_S\beta x^{\alpha_s}\right)^{-1}}\right)xdx\right) \\ &= \exp\left(-2\pi\lambda_S\int_{\rho_S(x)}^{\infty}\left(\frac{(-j\omega)P_S\beta x^{-\alpha_s}}{1+(-j\omega)P_S\beta x^{-\alpha_s}}\right)xdx\right), \end{aligned} \quad (55)$$

where (a) follows from $h_{S,i} \sim \exp(1)$, and $\rho_S(x)$ is the distance between a typical UE and the closet interfering SBSs. In (53), $L_{I_U^{dl}}(-j\omega)$ is calculated as

$$
\begin{aligned}
&L_{I_U^{dl}}(-j\omega)\\
&=\mathrm{E}\left\{e^{-(-j\omega)I_U^{dl}}\right\}=\mathrm{E}\left\{e^{-(-j\omega)\sum\limits_{X_{U_j}\in\Phi_u/X_{U_0}}\mathrm{E}\left\{P_{U_j}\right\}\beta g_{u_j}\left\|X_{U_j}\right\|^{-\alpha_s}}\right\}\\
&=\mathrm{E}_\Phi\left\{\exp\left(-(-j\omega)\sum_{X_{U_j}\in\Phi_{u/X_{U_0}}}\mathrm{E}\left\{P_{U_j}\right\}\beta g_{u_j}\left\|X_{U_j}\right\|^{-\alpha_s}\right)\right\}\\
&=\mathrm{E}_\Phi\left\{\prod_{X_{U_j}\in\Phi_{u/X_{U_0}}}\exp\left(-(-j\omega)\mathrm{E}\left\{P_{U_j}\right\}\beta g_{u_j}\left\|X_{U_j}\right\|^{-\alpha_s}\right)\right\}\\
&\overset{(a)}{=}\exp\left(-2\pi\lambda_S\left(\Lambda_M+\Lambda_{S^{dl}}\right)\right.\\
&\left.\int_0^\infty\left(1-\mathrm{E}_h\left\{\exp\left(-(-j\omega)\mathrm{E}\left\{P_{U_j}\right\}\beta g_{u_j}\left\|X_{U_j}\right\|^{-\alpha_s}\right)\right\}\right)udu\right)\\
&\overset{(b)}{=}\exp\left(-2\pi\lambda_S\left(\Lambda_M+\Lambda_{S^{dl}}\right)\right.\\
&\qquad\left.\times\int_0^\infty\left(\frac{1}{1+\left((-j\omega)\mathrm{E}\left\{P_{U_j}\right\}\beta u^{\alpha_s}\right)^{-1}}\right)udu\right)\\
&=\exp\left(-2\pi\lambda_S\left(\Lambda_M+\Lambda_{S^{dl}}\right)\right.\\
&\qquad\left.\times\int_0^\infty\left(\frac{(-j\omega)\mathrm{E}\left\{P_{U_j}\right\}\beta u^{-\alpha_s}}{1+(-j\omega)\mathrm{E}\left\{P_{U_j}\right\}\beta u^{-\alpha_s}}\right)udu\right),
\end{aligned}
\tag{56}
$$

where (a) represent the density of the FD UEs depends on the serving BS in DL, and (b) follows from $g_{u_j} \sim \exp(1)$. After some manipulation, with substituting (56), (55), and (54) into (53), (53) into (52), and plugging (52) into (51) we obtained (30).

REFERENCES

[1] Y. Shi, E. Alsusa and M. W. Baidas, "Joint DL/UL decoupled cell-association and resource allocation in D2D-underlay HetNets," *IEEE Trans. Veh. Technol*., vol. 70, no. 4, pp. 3640-3651, Apr. 2021.

[2] A. Al-Fuqaha, M. Guizani, M. Mohammadi, M. Aledhari, and M. Ayyash, "Internet of things: A survey on enabling technologies, protocols, and applications," *IEEE Commun. Surv. Tutor*., vol. 17, no. 4, pp. 2347–2376, Fourthquarter 2015.

[3] T. Qiu, N. Chen, K. Li, M. Atiquzzaman, and W. Zhao, "How can heterogeneous internet of things build our future: A survey," *IEEE Commun. Surv. Tutor*., vol. 20, no. 3, pp. 2011–2027, thirdquarter 2018.

[4] L. Chettri and R. Bera, "A comprehensive survey on internet of things (IoT) toward 5G wireless systems," *IEEE Internet of Things J*., vol. 7, no. 1, pp. 16–32, Jan. 2020.

[5] D. Xu and H. Zhu, "Secure transmission for SWIPT IoT systems with full-duplex IoT devices," *IEEE Internet of Things J*., vol. 6, no. 6, pp. 10915–10933, Dec. 2019.

[6] T. Lv, H. Gao, Z. Shi and X. Su, "Energy efficiency of two-tier heterogeneous networks with energy harvesting," in *Proc. IEEE ICC,* Paris. France, May 2017, pp. 1-6.

[7] I. Atzeni and M. Kountouris, "Full-duplex MIMO small-cell networks with interference cancellation," *IEEE Trans. Wireless Commun.*, vol. 16, no. 12, pp. 8362–8376, Dec 2017.

[8] A. H. Sakr and E. Hossain, "On user association in multi-tier full-duplex cellular networks," *IEEE Trans. Commun*., vol. 65, no. 9, pp. 4080–4095, Sept. 2017.

[9] S. Akbar, Y. Deng, A. Nallanathan, M. Elkashlan, and G. K. Karagiannidis, "Massive multiuser MIMO in heterogeneous cellular networks with full duplex small cells," *IEEE Trans. Commun*., vol. 65, no. 11, pp. 4704– 4719, Nov. 2017.

[10] P. Anokye, R. K. Ahiadormey, C. Song, and K. Lee, "On the sum-rate of heterogeneous networks with low-resolution ADC quantized full-duplex massive MIMO-enabled backhaul," *IEEE Wireless Commun.* Lett., vol. 8, pp. 452–455, Apr. 2019.

[11] M. Mohammadi, H. A. Suraweera, Y. Cao, I. Krikidis, and C. Tellambura, "Full-duplex radio for uplink/downlink wireless access with spatially random nodes," *IEEE Trans. Commun*., vol. 63, no. 12, pp. 5250–5266, Dec. 2015.

[12] M. Duarte, C. Dick, and A. Sabharwal, "Experiment-driven characterization of full-duplex wireless systems," *IEEE Trans. Wireless Commun.*, vol. 11, no. 12, pp. 4296–4307, Dec. 2012.

[13] M. Mohammadi, H. A. Suraweera, and C. Tellambura, "Uplink/downlink rate analysis and impact of power allocation for full-duplex cloud-RANs," *IEEE Trans. Wireless Commun.*, vol. 17, no. 9, pp. 5774–5788, Sept. 2018.

[14] M. Bacha, Y. Wu, and B. Clerckx, "Downlink and uplink decoupling in two-tier heterogeneous networks with multi-antenna base stations," *IEEE Trans. Wireless Commun*., vol. 16, no. 5, pp. 2760–2775, May 2017.

[15] H. Elshaer, F. Boccardi, M. Dohler, and R. Irmer, "Downlink and uplink decoupling: A disruptive architectural design for 5G networks," in *Proc. IEEE GLOBECOM*, Austin, TX, USA, Dec. 2014, pp. 1798–1803.

[16] A. H. Sakr and E. Hossain, "On user association in multi-tier full-duplex cellular networks," *IEEE Trans. Commun*., vol. 65, no. 9, pp. 4080–4095, Sept. 2017.

[17] M. Bacha, Y. Wu, and B. Clerckx, "Downlink and uplink decoupling in two-tier heterogeneous networks with multi-antenna base stations," *IEEE Trans. Wireless Commun*., vol. 16, no. 5, pp. 2760–2775, May 2017.

[18] C. DAI, K. Zhu, C. Yi, and E. Hossain, "Decoupled uplink-downlink association in full-duplex cellular networks: A contract-theory approach," *IEEE Trans. Mobile Comput*., pp. 1–1, 2020.

[19] K. Sun, J. Wu, W. Huang, H. Zhang, H. Hsieh, and V. C. M. Leung, "Uplink performance improvement for downlink-uplink decoupled HetNets with non-uniform user distribution," *IEEE Trans. Veh. Technol*., vol. 69, pp. 7518–7530, July 2020.

[20] W. Liu, S. Jin, M. Matthaiou, and X. You, "Transmission scheme and performance analysis of multi-cell decoupled heterogeneous networks," *IEEE Trans. Commun*., vol. 68, no. 7, pp. 4423–4436, July 2020.

[21] I. S. Gradshteyn and I. M. Ryzhik, *Table of Integrals, Series and Products*, 7th ed. Academic Press, 2007.

[22] Y. Zhu, L. Wang, K. K. Wong, S. Jin, and Z. Zheng, "Wireless power transfer in massive MIMO-aided HetNets with user association*," IEEE Trans. Commun*., vol. 64, no. 10, pp. 4181–4195, Oct. 2016.

[23] C. Liu and H. Hu, "Full-duplex heterogeneous networks with decoupled user association: Rate analysis and traffic scheduling," *IEEE Trans. Commun*., vol. 67, no. 3, pp. 2084–2100, Mar. 2019.

[24] C. Liu and L. Wang, "Optimal cell load and throughput in green small cell networks with generalized cell association," *IEEE J. Sel. Areas Commun*., vol. 34, no. 5, pp. 1058–1072, May 2016.

[25] M. Mohammadi, B. K. Chalise, H. A. Suraweera, C. Zhong, G. Zheng, and I. Krikidis, "Throughput analysis and optimization of wireless-powered multiple antenna full-duplex relay systems," *IEEE Trans. Commun*., vol. 64, no. 4, pp. 1769–1785, Apr. 2016.

[26] S. Haghgoy, M. Mohammadi and Z. Mobini, "Performance analysis of decoupled UL/DL user association in wireless-powered massive MIMO-aided heterogeneous networks," in *Proc. IEEE Int. Conf. Internet of Things and Applications (IoT)*, Iran. Isfahan, May 2021, pp. 1-7.

[27] A. He, L. Wang, Y. Chen, K. Wong and M. Elkashlan, "Spectral and energy efficiency of uplink D2D underlaid massive MIMO cellular networks, " *IEEE Tran. Commun.*, vol. 65, no. 9, pp. 3780-3793, Sept. 2017.

Sepideh Haghgoy received the B.Sc.and the M.Sc. degrees in Electrical Engineering from the Shahrekord University, Iran, in 2018 and 2021, respectively. Her research interests are in the areas of Heterogeneous Networks, Wireless Power Transfer, Full-duplex Communication and Stochastic Geometry.

Mohammadali Mohammadi (S'09, M'15) received the B.Sc. degree in Electrical Engineering from the Isfahan University of Technology, Isfahan, Iran, in 2005, and the M.Sc. and Ph.D. degrees in Electrical Engineering from K. N. Toosi University of Technology, Tehran, Iran in 2007 and 2012, respectively. From November 2010 to November 2011, he was a visiting researcher in the Research School of Engineering, the Australian National University, Australia, working on Cooperative Networks. He is currently an Associate Professor in the Faculty of Engineering, Shahrekord University, Iran. His main research interests include Cooperative Communications, Energy Harvesting and Green Communications, Full-Duplex Communications, Cell-Free Massive MIMO and Stochastic Geometry.

Zahra Mobini (S'09, M'15) received the B.Sc. degree in Electrical Engineering from Isfahan University of Technology, Isfahan, Iran, in 2006, and the M.Sc. and Ph.D. degrees, both in Electrical Engineering, from the M. A. University of Technology and K. N. Toosi University of Technology, Tehran, Iran, respectively. From November 2010 to November 2011, she was a Visiting Researcher at the Research School of Engineering, Australian National University, Canberra, ACT, Australia. She is currently an Assistant Professor with the Faculty of Engineering, Shahrekord University, Shahrekord, Iran. Her research interests include Wireless Communication Systems, Cooperative Networks, Cell-free Massive MIMO and Network Coding.